

Strongly coupled near-field radiative and conductive heat transfer between planar objects

Riccardo Messina,^{1,*} Weiliang Jin,^{2,*} and Alejandro W. Rodriguez²

¹Laboratoire Charles Coulomb (L2C), UMR 5221 CNRS-Université de Montpellier, F- 34095 Montpellier, France

²Department of Electrical Engineering, Princeton University, Princeton, NJ 08544, USA

We study the interplay of conductive and radiative heat transfer (RHT) in planar geometries and predict that temperature gradients induced by radiation can play a significant role on the behavior of RHT with respect to gap sizes, depending largely on geometric and material parameters and not so crucially on operating temperatures. Our findings exploit rigorous calculations based on a closed-form expression for the heat flux between two plates separated by vacuum gaps d and subject to arbitrary temperature profiles, along with an approximate but accurate analytical treatment of coupled conduction–radiation in this geometry. We find that these effects can be prominent in typical materials (e.g. silica and sapphire) at separations of tens of nanometers, and can play an even larger role in metal oxides, which exhibit moderate conductivities and enhanced radiative properties. Broadly speaking, these predictions suggest that the impact of RHT on thermal conduction, and vice versa, could manifest itself as a limit on the possible magnitude of RHT at the nanoscale, which asymptotes to a constant (the conductive transfer rate when the gap is closed) instead of diverging at short separations.

Two non-touching bodies held at different temperatures can exchange heat through photons. In the far field, i.e. separations $d \gg$ thermal wavelength $\lambda_T = \hbar c/k_B T$ (of the order of $8 \mu\text{m}$ at room temperature), the maximum radiative heat transfer (RHT) between them is limited by the well-known Stefan–Boltzmann law [1]. In the near field, i.e. $d \ll \lambda_T$, evanescent waves can tunnel and contribute flux, enabling RHT to exceed this limit by several orders of magnitude [2–4]. Such enhancements can be larger in nano-structured surfaces [5, 6], but only a handful of these have been studied thus far [7–10], leaving much room for improvements [5]. A more commonly studied heat-transport mechanism is thermal conduction, involving transfer of energy through phonons or electrons. Although conduction is typically more efficient than RHT [11–13], there are ongoing theoretical and experimental efforts aimed at discovering novel materials and structures leading to larger RHT, with recent work suggesting the possibility of orders of magnitude enhancements [5], in which case RHT could not only compete but even exceed conduction in situations typically encountered in everyday experiments (e.g. under ambient conditions).

In this paper, we present an approach for studying coupled conduction–radiation (CR) problems between planar objects separated by gaps that captures the full interplay of near-field RHT and thermal conduction at the nanoscale. Using an exact, closed-form expression of the slab–slab RHT in the presence of arbitrary temperature distributions, we show that CR interplay can give rise to significant temperature gradients and thereby greatly modify RHT, causing the latter to asymptote to a constant, the conductive flux when the gap is closed, which sets a fundamental limit to radiative heat exchange at short separations. We provide evidence of the validity of a simple but useful surface–sink approximation that treats the impact of RHT on conduction as arising purely at the vacuum–slab interfaces, yielding analytical expressions with which one can study the scaling behavior and impact of these effects with respect to relevant parameters. For instance, we find that their prominence is largely independent of operating temperatures but strongly tied to the choice of materials (e.g. glasses

and oxides versus highly conductive metals) and geometries (e.g. thin versus macroscopic films). Furthermore, these phenomena lie within the reach of current-generation experiments [14], leading to significant changes in RHT between typical materials like silica and sapphire at relatively large gap sizes \sim several tens of nanometers, and potentially playing an even greater role in metal oxides, which exhibit low-loss infrared polaritons [15, 16] and therefore enhance RHT.

Coupled photonic and phononic diffusion processes in nanostructures are becoming increasingly important [17, 18]. While recent works have primarily focused on the interplay between thermal diffusion and external optical illumination, e.g. laser-induced, localized heating of plasmonic structures [19–23], the thermal radiation emitted by a heated body and absorbed by nearby objects can also be a great source of heating or cooling. To date, however, the impact of RHT on conduction remains largely unexplored, with the consensus view being that radiation is insufficiently large to result in appreciable temperature gradients [12, 13, 24]. On the other hand, modern experiments measuring RHT between planar surfaces are beginning to probe the nanometer regime [14, 25–37], and in certain cases offer evidence of deviations from the typical $1/d^2$ behavior associated with near-field enhancement [38, 39] at nanometric distances, often attributed to non-local [17, 40] or phonon-tunneling [18] effects. Here, we find that depending on geometric configuration and materials, radiation-induced temperature gradients can play a significant role on transport above the nanometer regime, requiring a full treatment of the coupling between conduction and radiation.

Exact formulation of coupled conduction–radiation.— In what follows, we present a formulation of coupled CR applicable to the typical situation of two planar bodies (the same framework can be extended to multiple bodies), labelled a and b , separated by a gap of size d . We assume that the slabs exhibit arbitrary temperature profiles and exchange heat among one other. Neglecting convection and considering bodies with lengthscales larger or of the order of their phonon mean-free path, in which case Fourier conduction is valid, the stationary temperature distribution satisfies the one-dimensional coupled

CR equation:

$$\frac{\partial}{\partial z} \left[\kappa(z) \frac{\partial T(z)}{\partial z} \right] + \int dz' \varphi(z', z) = Q(z), \quad (1)$$

where $\kappa(z)$ and $Q(z)$ represent the bulk Fourier conductivity and external heat-flux rate at z , respectively, while $\varphi(z', z)$ denotes the radiative power per unit volume from a point z' to z . Previous studies of (1) considered only radiative energy escaping into vacuum through the surfaces of the objects, exploiting simple, albeit inaccurate ray-optical approximations that are inapplicable for sub-wavelength objects or in the near field [11, 41]. The novelty of our approach to (1) is that φ , as written above and computed below, is fundamentally tied to accurate and modern descriptions of RHT based on macroscopic fluctuational EM [2, 42], allowing us to explore regimes (e.g. distances $\ll \lambda_T$) where near-field effects dominate RHT among different objects. In particular, as we show below, in some regimes RHT can lead to observable temperature distributions. Although we only consider the impact of external radiation on the temperature profile and vice versa, under large temperature gradients, RHT could potentially modify the intrinsic thermal conductivity of these objects [17, 43, 44], a situation that we leave to future work. We also ignore far-field radiation since it is negligible compared to conduction or RHT at the distances considered in this work.

We focus on the scenario illustrated on the inset of Fig. 1, in which the temperature of slab a (b) slab is fixed at T_L (T_R) by means of a thermostat, except for a region of thickness t_a (t_b). To study this problem, we calculate the RHT via a Fourier expansion of the slabs' scattering matrices [45]. Such techniques were recently employed to obtain close-formed analytical expressions of RHT between plates of uniform temperature [46–49]. Here, we extend these results to consider the more general problem of slabs under arbitrary temperature distributions. Toward this aim, we generalize prior methods [47, 49] by dividing each slab into films of infinitesimal thicknesses, each having a fixed temperature. Describing the associated EM fields at each point by means of the fluctuation-dissipation theorem (from which the RHT can be deduced), and considering multiple reflections associated with the various interfaces, we find that the evanescent RHT per unit volume from a point z_a in slab a to a point z_b in slab b , $\varphi(z_a, z_b) = \int_0^\infty d\omega \int_{\omega/c}^\infty d\beta \varphi_a(\omega, \beta; z_a, z_b)$, can be expressed analytically in the closed form [50]:

$$\begin{aligned} \varphi(\omega, \beta; z_a, z_b) &= \frac{4\beta}{\pi^2} (r'' k''_{zm})^2 \frac{e^{-2k''_z d} e^{-2k''_{zm}(z_b-d/2)}}{|1 - r^2 e^{-2k''_z d}|^2} \\ &\times \left(N[\omega, T(z_a)] - N[\omega, T(z_b)] \right), \end{aligned} \quad (2)$$

where β denotes the conserved, parallel (x - y) wavevector $k_z = \sqrt{\omega^2/c^2 - \beta^2}$ and $k_{zm} = \sqrt{\varepsilon\omega^2/c^2 - \beta^2}$ the perpendicular wavevectors in vacuum and the interior of the slabs, respectively, and where we introduced the transverse-magnetic (dominant) polarization Fresnel reflection coefficient of a planar ε -vacuum interface, $r = (\varepsilon k_z - k_{zm})/(\varepsilon k_z + k_{zm})$. Note

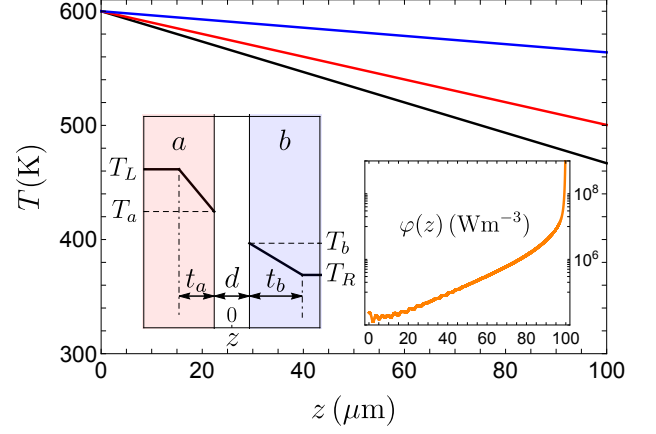


FIG. 1. The left inset shows a schematic of two parallel slabs separated by a distance d along the z direction ($z = 0$ denotes the middle of the gap). The two slabs exhibit a temperature profile $T(z)$: the temperature is constant and has values T_L and T_R in the regions $z \leq -d/2 - t_a$ and $z \geq d/2 + t_b$, respectively, and variable in the regions $-d/2 - t_a < z < -d/2$ and $d/2 < z < d/2 + t_b$, with T_a and T_b denoting the temperatures at the slab–vacuum interfaces. In the main part of the figure, temperature profile along the temperature-varying region of the hot slab in a configuration involving two silica slabs with $t_a = t_b = 100 \mu\text{m}$ held at external temperatures $T_L = 600 \text{ K}$ and $T_R = 300 \text{ K}$ at the outer ends, and separated by vacuum gaps d . The points $z = 0, 100 \mu\text{m}$ represent the boundary of the thermostat and the interface with the vacuum gap. The three lines correspond to $d = 10 \text{ nm}$ (black), 20 nm (red) and 50 nm (blue). The right inset shows the z -dependent radiative flux-rate $\varphi(z_a)$ (see text) along slab a at $d = 100 \text{ nm}$.

that we restrict our analysis to the transverse-magnetic polarization because only it supports a surface phonon-polariton resonance. Equation (2) permits fast solutions of coupled CR problems in this geometry for a wide range of parameters.

Surface–sink approximation: At small separations, near-field RHT is dominated by large- β surface modes that are exponentially confined to the slab–vacuum interfaces [4]. Hence, it is sufficient (as discussed below and confirmed through exact results in Fig. 1) to treat its impact on conduction as a purely surface effect, in which case the entire problem can be described through the surface temperatures. In particular, under this assumption, given a distance d , identical conductivities κ and temperature-varying regions $t = t_a = t_b$, and external temperatures T_L and T_R , the only unknowns are the interface temperatures T_a and T_b , which satisfy the following boundary conditions:

$$-\kappa \frac{T_a - T_L}{t} = -\kappa \frac{T_R - T_b}{t} = \varphi, \quad (3)$$

Here, φ denotes the net heat exchanged between the two slabs (assumed to take place at the surfaces), whose spectral ω and

β components are given by [50]:

$$\begin{aligned} \varphi(\omega, \beta) = & \frac{2\beta}{\pi^2} (r'')^2 k''_{zm} \frac{e^{-2k''_z d}}{|1 - r^2 e^{-2k''_z d}|^2} \int_0^{+\infty} dz e^{-2k''_{zm} z} \\ & \times \left(N[\omega, T(-d/2 - z)] - N[\omega, T(d/2 + z)] \right). \end{aligned} \quad (4)$$

Despite the complex dependence of the heat flux on separation and temperature profile, we find that it is possible to approximate the former using a simple, power-law expression of the form, $\varphi \simeq h_0(T_a - T_b)/d^2$ [39] (valid as long as the radiation is primarily coming from the surface of the slabs), with the coefficient h_0 calculated as the near-field heat flux between two uniform-temperature slabs held at T_L and T_R , divided by $T_L - T_R$. Essentially, while the dependence of RHT on absolute temperature is generally nonlinear, the fact that conduction through the interior of the slabs scales linearly with $T_a - T_b$ and that energy must be conserved (i.e. changes in conductive transfer must be offset by corresponding changes in RHT), implies that φ must also scale linearly with $T_a - T_b$, with the precise value of the coefficient h_0 determined from the radiative conductivity at large values of d where radiation does not impact conduction. Given these simplifications, Eq. (3) can be solved to yield:

$$\frac{T_a - T_b}{T_L - T_R} = \left(1 + \frac{2th_0}{\kappa d^2} \right)^{-1}, \quad \frac{\varphi}{T_L - T_R} = \frac{h_0}{d^2} \left(\frac{T_a - T_b}{T_L - T_R} \right). \quad (5)$$

These formulas reveal that the interplay of conduction and radiation causes $T_a - T_b \rightarrow 0$ quadratically with d , producing a continuous temperature profile and leading to a finite value of $\varphi \rightarrow \kappa(T_L - T_R)/2t$ as $d \rightarrow 0$, the conductive flux through a gapless slab of thickness $2t$ subject to a linear temperature gradient $T_L - T_R$ (as it must, from energy conservation). Below, we show that the existence of such temperature gradients along with deviations from the typical $1/d^2$ RHT power law are within the reach of present experimental detection.

Numerical predictions.— To begin with, we first address the validity of the surface–sink approximation above. In order to do so, we of course need to consider the full coupled CR problem described by (1), requiring numerical evaluation of the spatial heat transfer $\varphi(z_a, z_b)$ in (2). For concreteness, we consider a practical situation typical of RHT experiments, involving two silica (SiO_2) slabs subject to external temperatures $T_L = 600$ K and $T_R = 300$ K by a thermostat at distance $t = t_a = t_b = 100 \mu\text{m}$ away from the slab–vacuum interfaces. Silica not only has relatively low $\kappa \approx 1.4$ W/m·K but also supports polaritonic resonances at mid-infrared wavelengths and has well-tabulated optical properties [51]. Figure 1 illustrates the increasing, *linear* temperature gradient present in slab a with decreasing separations d , a consequence of the exponential decay of the spatial heat transfer, $\varphi(z_a) = \int dz_b \varphi(z_b, z_a)$, illustrated on the inset at a fixed $d = 100$ nm. Results obtained through (5), with $h_0 = 5.53 \times 10^{-12}$ W/K, are in almost perfect (essentially indistinguishable) agreement with those of the full CR treatment and are therefore not shown. The same is

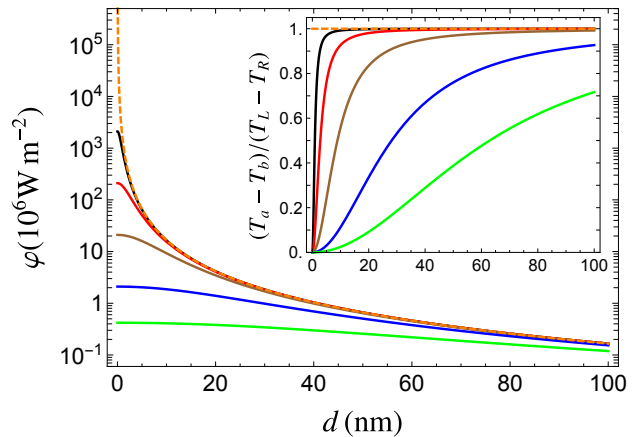


FIG. 2. Total flux φ and temperature difference $T_a - T_b$ (inset) as a function of distance d between two silica slabs (shown schematically on the left inset of Fig. 1) that are being held at $T_L = 600$ K and $T_R = 300$ K. The various solid lines correspond to different temperature-varying regions t (from top to bottom): 100 nm (black), 1 μm (red), 10 μm (brown), 100 μm (blue) and 500 μm (green). The orange dashed line shows φ in the absence of temperature gradients.

true at smaller values of t , down to tens of nanometers, below which the surface–sink approximation begins to fail.

Figure 2 shows φ and $T_a - T_b$ (inset), normalized by the external temperature difference $T_L - T_R$, as a function of d and for the same slab configuration but considering multiple $t = \{0, 0.1, 1, 10, 100, 500\} \mu\text{m}$, with decreasing values of t leading to smaller temperature gradients and larger φ . Here, $t = 0$ (dashed line) corresponds to the typical scenario where conduction dominates and hence there are no temperature gradients, in which case $\varphi = h_0(T_L - T_R)/d^2$ exhibits the expected divergence. Quite interestingly, we find that at typical values of $t = 100 \mu\text{m}$, the flux decreases by $\approx 50\%$ at distances $d \approx 30$ nm, well within the reach of current experiments [14, 25, 34–36]. This result may be particularly relevant to recent experiments [14] investigating RHT between large silica objects, which indicate deviations from the $1/d^2$ scaling behavior (along with flux saturation) at similar distances.

We now explore the degree to which these saturation effects depend on the choice of material and operating conditions, quantified via the separation regime at which they become significant. In particular, inspection of (5) allows us to define the distance $\tilde{d} = \sqrt{2th_0/\kappa}$ at which $T_a - T_b = \frac{1}{2}(T_L - T_R)$ and $\varphi = \frac{1}{2}h_0(T_L - T_R)/\tilde{d}^2$, corresponding to half the value of the RHT obtained when conduction and radiation do not influence one another. Figure 3 shows \tilde{d} as a function of the material-dependent ratio h_0/κ for the particular choice of $T_L = 600$ K, $T_R = 300$ K, and $t = 100 \mu\text{m}$, highlighting the square-root dependence of the former on the latter. Superimposed are the expected \tilde{d} associated with various materials of possible experimental interest (solid circles), obtained by employing appropriate values of κ and h_0 , which depend primarily on the

choice of external temperature. Within the surface–sink approximation (valid here), the latter do not influence the scaling of either φ or $T_a - T_b$ with respect to separation, as evident from (5). The inset of Fig. 3 shows h_0 as a function T_L for SiC, SiO₂, and aluminum zinc oxide (AZO), identified by their increasing values of h_0 , illustrating the near constancy of the coefficient over a wide range of acceptable temperature differences. Note that we consider unrealistically large values of T_L only to illustrate asymptotic behavior.

Noticeably, despite small differences in the value of h_0 between various materials, there are striking variations in \tilde{d} , which can range anywhere from a few nanometers in the case of SiC and GaAs, up to several tens of nanometers for SiO₂ and AZO, respectively. Such variations are almost entirely due to differences in thermal conductivities, which naturally play a major role in this problem, with the conductivities of SiC, SiO₂, and AZO taken to be $\kappa \simeq 120$ W/m·K, 1.4 W/m·K, and 1.2 W/m·K, respectively. Note that, generally, zinc oxides exhibit moderate values of thermal conductivities at high temperatures, depending on their fabrication method, with the value here taken from Ref. 52. The open circle in Fig. 3 indicates the expected $\tilde{d} \sim$ hundreds of nanometers associated with ultra-low conductivity ($\kappa \lesssim 0.05$ W/m·K) nanocomposite oxides that can now be engineered [15, 52, 53] and which are likely to play a more prominent role in future thermal devices [16]. We stress that our predictions are consistent with the lack of gradient effects observed in recent experiments involving materials such as silicon and Au, which exhibit low and high values of h_0 and κ , respectively. The case of silica is particularly interesting, however, since it is typically used in RHT experiments, yet the possibility of temperature gradients has never been considered. These results along with (5) can serve as a reference for future experiments, allowing estimates of the regimes under which these effects become relevant.

While our analysis above is based on the assumption of vacuum gaps, it is straightforward to generalize Eq. (5) to include the possibility of finite intervening conductivities, $\kappa_0 > 0$, requiring only that h_0 be replaced with $h_0 + \kappa_0 d$ in the first expression of Eq. (5). We find, however, that similar conclusions follow for small but finite $\kappa_0 \lesssim 10^{-5}$ W/m·K (typical of RHT experiments).

In conclusion, we have presented a study of coupled conduction–radiation heat transfer between planar objects at short distances. We have expressed the resulting temperature gradients and radiative-flux modifications in terms of simple, analytical expressions involving geometric and material parameters, showing that in systems well within experimental reach or already considered in experiments [14], both temperature gradients and flux saturation should be observed. A similar saturation phenomenon has been predicted to occur due to non-local damping [17, 40] and/or phonon-tunneling below the nanometer scale [18] (note that at atomistic scales where continuum electrodynamics fails, the boundary between phonon and radiative conduction is blurred). Our work suggests that even at and above nano-meter gaps, and depending on material and geometric conditions, CR interplay could

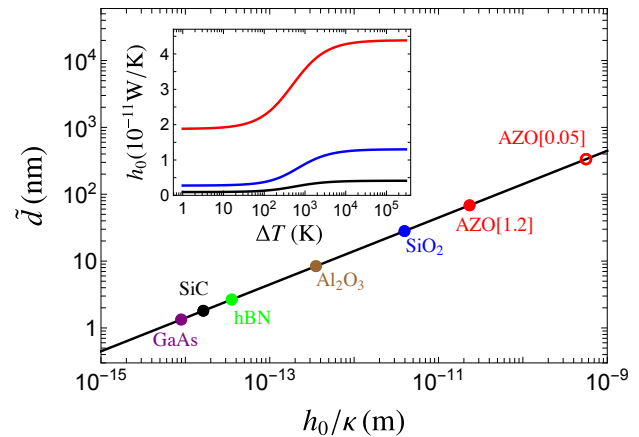


FIG. 3. Typical distance scale \tilde{d} relevant to conduction–radiation problems (see text) as a function of the material-dependent ratio h_0/κ for two slabs with $t_a = t_b = 100 \mu\text{m}$. Solid circles denote corresponding values for specific material choices (abbreviations), with AZO[1.2] and AZO[0.05] denoting aluminum zinc oxides of different conductivities $\kappa = 1.2$ W/m·K [52] and potential $\kappa = 0.05$ W/m·K [15], respectively. The inset shows the dependence of the radiative-heat transfer coefficient h_0 on the external temperature gradient $\Delta T = T_L - 300$ K, for three cases, AZO (red), silica (blue) and SiC (black), with decreasing values.

instead become the dominant mechanism limiting RHT. Furthermore, there are significant efforts underway aimed at exploring regimes, e.g. smaller gap sizes or materials and structures leading to larger RHT (for applications in nanoscale cooling [54] and other thermal devices [55]), where these effects may be observed at even at larger separations. Our ongoing work generalizing the coupled CR formulation to arbitrary geometries reveals even larger interplay in structured surfaces [56, 57]. Arguably, advances in either or both directions will make such analyses necessary.

Acknowledgements This work was supported by the National Science Foundation under Grant no. DMR-1454836 and by the Princeton Center for Complex Materials, a MR-SEC supported by NSF Grant DMR 1420541.

* These authors contributed equally to this work.

- [1] J. R. Howell, M. P. Mengüç, and R. Siegel, *Thermal radiation heat transfer* (CRC press, 2010).
- [2] S. Basu, Z. Zhang, and C. Fu, *International Journal of Energy Research* **33**, 1203 (2009).
- [3] A. Volokitin and B. N. Persson, *Rev. Mod. Phys.* **79**, 1291 (2007).
- [4] K. Joulain, J.-P. Mulet, F. Marquier, R. Carminati, and J.-J. Greffet, *Surf. Sci. Rep.* **57**, 59 (2005).
- [5] O. D. Miller, S. G. Johnson, and A. W. Rodriguez, *Phys. Rev. Lett.* **115**, 204302 (2015).
- [6] C. Khandekar, W. Jin, O. D. Miller, A. Pick, and A. W. Rodriguez, preprint arXiv:1511.04492 (2015).

- [7] A. Narayanaswamy and G. Chen, Phys. Rev. B **77**, 075125 (2008).
- [8] M. Kruger, T. Emig, and M. Kardar, Phys. Rev. Lett. **106**, 210404 (2011).
- [9] A. P. McCauley, M. H. Reid, M. Kruger, and S. G. Johnson, Phys. Rev. B **85**, 165104 (2012).
- [10] A. W. Rodriguez, M. H. Reid, and S. G. Johnson, Phys. Rev. B **88**, 054305 (2013).
- [11] J. Holman, *Heat transfer* (McGraw-Hill Inc, 2010).
- [12] B. T. Wong, M. Francoeur, and M. P. Mengüç, International Journal of Heat and Mass Transfer **54**, 1825 (2011).
- [13] J. Z.-J. Lau, V. N.-S. Bong, and B. T. Wong, J. Quant. Spectrosc. Radiat. Transfer **171**, 39 (2016).
- [14] S. Shen, A. Narayanaswamy, and G. Chen, Nano Letters **9**, 2909 (2009).
- [15] C. Chiritescu, D. G. Cahill, N. Nguyen, D. Johnson, A. Bodapati, P. Keblinski, P. Zschack, Science **315**, 351 (2007).
- [16] D. G. Cahill, P. V. Braun, G. Chen, D. R. Clarke, S. Fan, K. E. Goodson, P. Keblinski, W. P. King, G. D. Mahan, A. Majumdar, Applied Physics Reviews **1**, 011305 (2014).
- [17] K. Joulain, J. Quant. Spectrosc. Radiat. Transfer **109**, 294 (2008).
- [18] V. Chiloyan, J. Garg, K. Esfarjani, and G. Chen, Nature Communications **6**, 6775 (2015).
- [19] G. Baffou, C. Girard, and R. Quidant, Phys. Rev. Lett. **104**, 136805 (2010).
- [20] G. Baffou, E. B. Urea, P. Berto, S. Monneret, R. Quidant, and H. Rigneault, Nanoscale **6**, 8984 (2014).
- [21] H. Ma, P. Tian, J. Pello, P. M. Bendix, and L. B. Oddershede, Nano Letters **14**, 612 (2014).
- [22] C. L. Baldwin, N. W. Bigelow, and D. J. Masiello, The journal of physical chemistry letters **5**, 1347 (2014).
- [23] R. Biswas and M. L. Povinelli, ACS Photonics **2**, 1681 (2015).
- [24] B. T. Wong, M. Francoeur, V. N.-S. Bong, and M. P. Mengüç, J. Quant. Spectrosc. Radiat. Transfer **143**, 46 (2014).
- [25] A. Kittel, W. Müller-Hirsch, J. Parisi, S.-A. Biehs, D. Reddig, and M. Holthaus, Phys. Rev. Lett. **95**, 224301 (2005).
- [26] A. Narayanaswamy, S. Shen, and G. Chen, Phys. Rev. B **78**, 115303 (2008).
- [27] L. Hu, A. Narayanaswamy, X. Chen, and G. Chen, Appl. Phys. Lett. **92**, 133106 (2008).
- [28] E. Rousseau, A. Siria, G. Joubran, S. Volz, F. Comin, J. Chevrier, and J.-J. Greffet, Nature Photon. **3**, 514 (2009).
- [29] R. S. Ottens, V. Quetschke, S. Wise, A. A. Alemi, R. Lundock, G. Mueller, D. H. Reitze, D. B. Tanner, and B. F. Whiting, Phys. Rev. Lett. **107**, 014301 (2011).
- [30] T. Kralik, P. Hanzelka, V. Musilova, A. Srnka, and M. Zobac, Rev. Sci. Instrum. **82**, 055106 (2011).
- [31] T. Kralik, P. Hanzelka, M. Zobac, V. Musilova, T. Fort, and M. Horak, Phys. Rev. Lett. **109**, 224302 (2012).
- [32] P. J. van Zwol, L. Ranno, and J. Chevrier, Phys. Rev. Lett. **108**, 234301 (2012).
- [33] P. J. van Zwol, S. Thiele, C. Berger, W. A. de Heer, and J. Chevrier, Phys. Rev. Lett. **109**, 264301 (2012).
- [34] B. Song *et al.*, Nature Nanotechnology **10**, 253 (2015).
- [35] K. Kim *et al.*, Nature **528**, 387 (2015).
- [36] K. Kloppstech *et al.*, preprint arXiv:1510.06311 (2015).
- [37] R. St-Gelais, L. Zhu, S. Fan, and M. Lipson, Nature Nanotechnology **11**, 515 (2016).
- [38] P.-O. Chapuis, S. Volz, C. Henkel, K. Joulain, and J.-J. Greffet, Phys. Rev. B **77**, 035431 (2008).
- [39] J.-P. Mulet, K. Joulain, R. Carminati, and J.-J. Greffet, Microscale Thermophysical Engineering **6**, 209 (2002).
- [40] C. Henkel and K. Joulain, Appl. Phys. B **84**, 61 (2006).
- [41] R. M. S. da Gama, Applied Mathematical Modelling **28**, 795 (2004).
- [42] S. M. Rytov, Y. A. Kravtsov, and V. I. Tatarskii, *Principles of Statistical Radiophysics* (Springer, Berlin, 1988).
- [43] D.-Z. A. Chen, A. Narayanaswamy, and G. Chen, Phys. Rev. B **72**, 155435 (2005).
- [44] S. Volz, *et al.*, The Eur. Phys. J. B **89**, 1 (2016).
- [45] M. Francoeur, M. P. Mengüç, and R. Vaillon, J. Quant. Spectrosc. Radiat. Transfer **110**, 2002 (2009).
- [46] P. Ben-Abdallah, K. Joulain, J. Drevillon, and G. Domingues, J. Appl. Phys. **106**, 044306 (2009).
- [47] R. Messina and M. Antezza, Phys. Rev. A **84**, 042102 (2011).
- [48] R. Messina, M. Antezza, and P. Ben-Abdallah, Phys. Rev. Lett. **109**, 244302 (2012).
- [49] R. Messina and M. Antezza, Phys. Rev. A **89**, 052104 (2014).
- [50] R. Messina, W. Jin, and A. W. Rodriguez, in preparation.
- [51] *Handbook of Optical Constants of Solids*, edited by E. Palik (Academic Press, New York, 1998).
- [52] J. Loureiro *et al.*, J. Mater. Chem. A **2**, 6649 (2014).
- [53] P. Jood, R. J. Mehta, Y. Zhang, G. Peleckis, X. Wang, R. W. Siegel, T. Borca-Tasciuc, S. X. Dou, and G. Ramanath, Nano Letters **11**, 4337 (2011).
- [54] B. Guha, C. Otey, C. B. Poitras, S. Fan, and M. Lipson, Nano Letters **12**, 4546 (2012).
- [55] P. Ben-Abdallah and S.-A. Biehs, AIP Advances **5**, 053502, (2015).
- [56] A. G. Polimeridis, M. T. H. Reid, W. Jin, S. G. Johnson, J. K. White, and A. W. Rodriguez, Phys. Rev. B **92**, 134202 (2015).
- [57] W. Jin, R. Messina, and A. W. Rodriguez, in preparation.